

1  
2  
3  
4

5 *Title:*

6 **Discharge measurement with salt dilution method in irrigation canals: direct**  
7 **sampling and geophysical controls.**

8 *Authors:*

9 **Cesare Comina<sup>1</sup>, Manuela Lasagna<sup>1</sup>, Domenico Antonio De Luca<sup>1</sup> and Luigi**  
10 **Sambuelli<sup>2</sup>**

11 *Authors affiliation:*

12 <sup>1</sup> Dept. of Earth Science (DST), Università degli Studi di Torino, via Valperga Caluso,  
13 35, 10125 Italy;

14  
15 <sup>2</sup> Dept. of Environment, Land and Infrastructure Engineering (DIATI), Politecnico di  
16 Torino, corso Duca degli Abruzzi, 24, 10129 Italy;

17  
18

19

20

21 *keywords:*

22 canal discharge; salt dilution method; slug injection; sampling optimization; fast electric  
23 resistivity tomography.

24  
25  
26

27 **ABSTRACT**

28

29

30

31

32

33

34

35

36

37

38

39

40

41

42

43

44

45

46

47

48

49

An important starting point for designing management improvements, particularly in irrigation areas, is to record the baseline state of the water resources, including the amount of discharge from canals. In this respect discharge measurements by means of the salt dilution method is a traditional and well-documented technique. However, this methodology can be strongly influenced by the natural streaming characteristics of the canal (e.g. laminar versus turbulent flow) and accurate precautions must be considered in the choice of both the measuring section and the length of the measuring reach of the canal which can affect the plume shape. [These precautions can fight with logistical problems on real test sites \(i.e. accessibility of banks, length of appropriate reaches etc...\).](#) Therefore ~~T~~the knowledge of plume distribution in the measuring cross-section is of primary importance for a correct location of sampling points aimed in obtaining a reliable measurement. To obtain this, geophysical imaging of an NaCl plume from a slug-injection salt dilution test has been ~~performed~~ [attempted within this paper](#) by means of cross-flow fast electric resistivity tomography (FERT) in a real case history. Direct sampling of the same plume has been also performed with a [prototype](#) multisampling optimization technique to obtain an average value over the measuring section by means of contemporarily sampling water in nine points. [Preliminary R](#)results [of the single test presented](#) show that a ~~correct~~ visualization of the passage of the salt plume is possible by means of geophysical controls and that this can potentially help in the ~~correct~~ location of sampling points.

50           **INTRODUCTION**

51  
52  
53

54           Improved management of water resources is becoming more and more important  
55 as several areas of the world suffer from water shortages. An important starting point for  
56 designing management improvements is to record the baseline state of the resources,  
57 including the amount of discharge from watercourses. Discharge is therefore an  
58 important property and is frequently monitored along many of the major rivers, streams  
59 and canals. Discharge measurement by means of injection of a NaCl-solution and  
60 integration of the electrical conductivity (EC) as a function of time is a traditional and  
61 well-documented method (salt dilution method). Alternatives for a precise discharge  
62 measurement may be the use of a current meter or the float method (Kalbus et al., 2006).  
63 The salt dilution technique is, however, the mostly used method in open channels in  
64 investigating superficial flows, especially in remote mountainous or difficult to access  
65 areas where it can be hard to establish an high quality hydrologic profile, and even  
66 harder to measure actual flow speed (Radulović et al., 2008).

67           Within the salt dilution method, constant-rate injection of salt is best suited for  
68 small streams at low flows (discharges less than about 0.1 m<sup>3</sup>/s), conversely slug  
69 injection can be used to gauge flows up to 10 m<sup>3</sup>/s or greater, depending upon channel  
70 characteristics (Moore, 2005).

71           A limit of the salt dilution method is the amount of tracer to be added to increase  
72 the conductivity at the peak of the tracer flow-through curve. This is mainly linked to the  
background level of the conductivity: if this is less than 100 μS/cm a smaller amount of

73 salt per m<sup>3</sup> of runoff can be added; otherwise if the background conductivity is more  
74 than 500 μS/cm, more than 5 kg of salt per m<sup>3</sup> should be used (Gees, 1990). [More in](#)  
75 [general Kite \(1993\) suggests that peak EC should be 50% higher than background, while](#)  
76 [Hudson and Fraser \(2002\) suggest that peak EC should be at least 5 times higher than](#)  
77 [background. Moore \(2005\) proposes that increasing EC by 100–200% of background](#)  
78 [should be adequate for streams with low background EC \(less than about 50 μS/cm\),](#)  
79 [while Kite's \(1993\) guideline should be reasonable for streams with background EC](#)  
80 [greater than about 100 μS/cm.](#) However, given this limitation, an advantage of the  
81 method is that the measuring equipment is very easy to move. The salt can be dissolved  
82 on site in a vessel (bucket, barrel) and it can be directly poured from it. In this respect  
83 slug injection is more commonly used, as it requires no additional equipment. A  
84 disadvantage of this method is that only a runoff less than 4 m<sup>3</sup>/s can be made easily,  
85 because the amount of salt to be dissolved is difficult to handle (about 20 kg of salt for 4  
86 m<sup>3</sup>/s runoff) (Gees, 1990).

87 Under suitable conditions, streamflow measurements made by slug injection can  
88 be precise within about ±5% (Day, 1976). However, tracer-dilution method requires a  
89 complete vertical and lateral mixing at the sampling site that needs to be assessed,  
90 particularly in linear irrigation canals, like in the present case study. Vertical mixing is  
91 usually accomplished very rapidly compared to lateral mixing (Rantz, 1982).  
92 Frequently, long reaches are needed for complete lateral mixing of the tracer. The  
93 mixing distance will vary however also with the hydraulic characteristics of the reach  
94 (e.g. laminar versus turbulent flow). When the slug injection method is used, complete

95 mixing is considered to have occurred when the area under the concentration-time curve  
96 has the same value at all points in the downstream sampling section (Rantz, 1982).  
97 Generally, an optimum mixing length is the one that produces mixing adequate for an  
98 accurate discharge measurement but does not require an excessively long duration of  
99 sampling. [Several empirical equations can be found in literature to evaluate the mixing](#)  
100 [length \(e.g. Moore, 2005; Jaramillo, 2007\), taking into consideration different canal](#)  
101 [features \(gross estimated discharge, width, etc...\) and the type of tracer injected.](#) If  
102 adequate mixing is not known to exist at a given sampling site, the tracer cloud in the  
103 slug injection method must be sampled for its entire time of passage (from the time of its  
104 first appearance until the time of its disappearance) at several locations throughout the  
105 sampling cross section of the channel (Rantz, 1982). Experience indicates that regardless  
106 of method or stream size, at least three lateral sampling points should be used at each  
107 sampling site (Rantz, 1982).

108         Alternatively, to obtain a direct visualization of the tracer plume and then a  
109 proper location of the monitoring points, indirect geophysical measurements could be  
110 used, aimed at imaging the passage of the NaCl solution in the monitored section. In this  
111 respect process tomography, in the forms of electrical resistivity tomography (ERT) has  
112 been developed in the last decades of the 20<sup>th</sup> century as a tool for monitoring bi-phase  
113 or multi-phase mixtures flows in numerous applications (Xie et al., 1995; Tapp and  
114 Wilson, 1997). Tomographic methods, and their interpretation based on the electrical  
115 properties of water mixtures, are appealing in numerous [hydrogeological](#) applications  
116 since they can be used, for example, to image component concentration distributions and

117 detect transient dynamic changes in multi-phase processes. Moreover they can also give  
118 quantitative evaluations about the properties of imaged mixtures. In this respect various  
119 relationships can be found in the literature relating the electrical resistivity to the  
120 physico-chemical properties of the mixture.

121 Most of the applications of this technique (Fangary et al., 1998; Lucas et al.,  
122 (1999); Wang and Cilliers (1999); Yang and Liu (2000); Warsito and Fan (2001)) deal  
123 with cylindrical flows bodies (in pipes, cyclones, tanks) and the electrodes are placed on  
124 one or more circumferences orthogonal to the cylinder axis. This geometrical  
125 configuration assures an optimum conditioning of the inverse tomographic problem but  
126 however limits its applicability to real case studies on natural rivers or channels. Some  
127 previous studies have been already carried out assessing the possibility of recognising  
128 the presence of granular materials in slow water flows (Sambuelli et al., 2002) and in  
129 imaging solid and pollutants transport characteristics in fast water flows under  
130 laboratory conditions (Sambuelli and Comina, 2010) in situations where the imaged  
131 body cannot be entirely surrounded by electrodes as in the case of creeks, rivers and  
132 canals.

133 The objective of this study is therefore to ~~evidence-image~~ the ~~real~~ distribution of  
134 a NaCl plume from a slug-injection salt dilution test in a test cross section, by means of  
135 cross-flow fast electric resistivity tomography (FERT), and to compare the such  
136 obtained distribution with evaluate the effect that a non uniform tracer cloud could have  
137 on an incorrect location direct measurements of their localized monitoring points in the  
138 cross section. In this respect the application of the same technique presented in

139 | Sambuelli and Comina (2010) is reported in a ~~real~~-case history in order to monitor the  
140 | salt plume used for discharge measurement with the salt dilution method in slug  
141 | injection approach. A sampling optimization in the downstream sampling section was  
142 | also tested, sampling the canal water in different points of the cross section, and  
143 | obtaining an average value over the sampled area ~~by means of a contemporary water~~  
144 | ~~picking-up~~.

145

## 146 | MATERIAL AND METHODS

147 | After a brief introduction on the test site, the conceptual basis and field  
148 | procedures for slug injection using Salt Dilution method and geophysical controls are  
149 | hereafter exposed. Particularly the prototype water multi-sampling system, proposed for  
150 | the optimization of the tracer quantitative detection, is described together with the field  
151 | procedures necessary for the execution of electric tomographies.

152

### 153 | *THE STUDY AREA: THE OSASCO CANAL*

154 | The Osasco Canal is an irrigation canal located in Piedmont (north-western  
155 | Italy). It has an overall length of about 7 km and carries water from the Chisone River  
156 | (Figure 1). The investigated canal reach, in which direct measurements and geophysical  
157 | controls were made, has ~~a length of about 100 m~~, an average width of 2 m and about 0.5  
158 | m water level. The Osasco Canal has a gross average discharge of about 0.5 m<sup>3</sup>/s,  
159 | estimated with a current meter, and a water EC of about 170  $\mu$ S/cm (Clemente et alii,

2013; Perotti et alii, 2013). The EC, monitored in the canal, shows little variation during the day and it can be considered stable during the measuring time of the presented tests.

Given the natural variability of dimensions of the rectangular canal section and estimated average flow velocity, the flow regime of the canal can be considered to be “sinuous” with the meaning proposed by Scobey (1939): “a turbulent flow, according to Reynolds, but with a rather placid flow”.

Following preliminary calculations on the basis of literature empirical formulae (Moore, 2005; Jaramillo, 2007) the distance adequate to guarantee the complete mixing of the tracer resulted of about 50 m. In order to ensure an adequate testing length, a canal reach of 100 m was therefore chosen (Figure 1). ~~The Osaseo canal has a gross average discharge of 0.5 m<sup>3</sup>/s, estimated with a current meter, and a water EC of about 170 µS/cm (Clemente et alii, 2013; Perotti et alii, 2013).~~

Some pictures of both the sampling and the injection points are reported in Figure 2. In ~~this portion~~ the studied reach the bottom of the channel is cobbled (gravels and cobbles) and cement less except for a small portion immediately upstream of the chosen injection point, where a small cemented weir is located (Figure 2). The measuring section is located under a small road bridge and a canal curve is placed immediately downstream of this section (Figure 2). A part from injection and measuring sections the canal is difficult to access due to dense vegetation growing on the banks.

#### *CANAL REACH CHOICE*



182 Following precautions for the salt dilution method, the most appropriate canal  
183 reach has been selected for the execution of the tests (Figure 1 and Figure 2)  
184 considering that:

185 a) the reach should not have dead water between the injection and sampling  
186 points: the storage and slow release of tracer from those areas greatly prolongs the  
187 time required to the entire salt cloud to pass at the sampling site;

188 b) the sampling site has to be free of excessive turbulence; indeed EC  
189 measurements are adversely affected by the presence of air bubbles ~~(Figure 2)~~;

190 c) an injection point that is turbulent enough to ensure virtually instantaneous  
191 mixing is to be chosen; this condition is not always easy to be achieved especially in  
192 irrigation canals where laminar or sinuous flow can be predominating ~~(Figure 2)~~;

193 d) the background EC level of the river is to be stable during the measuring time;

194 e) it is important to identify an optimum mixing length for a given canal reach;  
195 too short distances will result in an inaccurate accounting of the tracer mass passing  
196 the sampling site, due to incomplete lateral mixing of the tracer, conversely, too great  
197 a distances will yield excellent results, but only if it is feasible to sample for a long  
198 enough period (Rantz, 1982).

199

## 200 *SLUG INJECTION METHOD WITH SAMPLING OPTIMIZATION*

201 The slug injection method required the instantaneous injection of a slug of tracer  
202 solution and the accounting of the total mass of tracer at the sampling cross section.  
203 Common salt (NaCl) was used as tracer; it is the most frequently used chemical tracer

204 and provides the best results (Drost, 1989; Kumar and Nachiappan, 2000; Tazioli, 2011).  
205 It indeed meets all the criteria for a tracer: is (a) 'chemically conservative', i.e., does not  
206 adsorb ('chemically bind') onto river sediments, (b) has a high solubility in water, (c) is  
207 relatively non-toxic, (d) can be measured in the field indirectly with a conductivity  
208 meter, and (e) is relatively cheap and readily available. In this study a NaCl mass of 9 kg  
209 was dissolved in a barrel within about 30 l of water and this slug was instantaneously  
210 injected into the canal at the injection point (Figure 2).

211 The slug of tracer solution instantaneously injected into the canal produced a  
212 concentration-time curve in the downstream sampling cross section. Given this  
213 experimental curve the equation for computing stream discharge, which is based on the  
214 principle of the conservation of mass, is (Rantz, 1982):

$$215 \quad Q = \frac{V_0 \cdot C_0}{\int_0^{\infty} (C - C_b) dt}$$

216 where Q is the discharge of the canal,  $V_0$  is the volume of the tracer solution injected  
217 into the canal,  $C_0$  is the concentration of this solution, C is the measured tracer  
218 concentration at a given time at the downstream sampling site and  $C_b$  is the background  
219 concentration of the canal.

220 The term  $\int_0^{\infty} (C - C_b) dt$  globally represents the total area under the concentration-  
221 time curve. To experimentally obtain this curve, the passage of the entire tracer cloud  
222 was monitored, by continuously measuring the EC value of the channel water at the  
223 sampling section, to determine the relationship between EC and time. The elapsed time

224 between subsequent measures of EC was 5 s. The basic principles is that the ion  
225 concentration of the slug injected increases the natural water concentration,  $(C - C_b)$  can  
226 be viewed as an "incremental" concentration with respect to the background,  
227 consequently increases also the measured electrical conductivity which can be used as  
228 an index of the salt concentration. Indeed, over a wide range of concentrations the EC is  
229 directly proportional to salt concentration (Radulović et al., 2008; Moore, 2005; Gees,  
230 1990; Rantz, 1982). The recorded values of EC were then transformed into  
231 concentration values through the use of a laboratory estimated calibration line. This  
232 calibration was constructed measuring the variation of EC in the water canal to the  
233 addition of different amounts of NaCl. In this way the "incremental concentration" in  
234 respect to the natural water conductivity, which is used as reference, is obtained. The  
235 example calibration line for the present study is reported in Figure 3 [showing an highly](#)  
236 [reliable fit to experimental data \( \$R^2\$  almost equal to unity\)](#).

237 Tracer-dilution measurements require a complete tracer mixing at the sampling  
238 site. However, the detection of the tracer is often performed in only one point, normally  
239 central to the sampling cross section. This procedure can create some mistakes in the  
240 calculation of canals' discharge if the injection solution is not fully mixed across the  
241 channel at the downstream sampling section.

242 In order to make the EC values more representative of the entire sampling cross  
243 section and to obtain the optimization of quantitative detection, a water multi-sampling  
244 system was devised. This system was realized by means of a framework of steel rods to  
245 which 9 tubes of small diameter are connected. The tubes are linked to a [single](#) water

246 | pump which spills the water of the canal simultaneously from the 9 measuring points  
247 | [and collect and compose all 9 samples in one average data point at each sample interval.](#)

248 | The objective of this apparatus is to allow for a more uniformly distributed sampling  
249 | points through the whole section of the canal; however due to the accessibility of the  
250 | measured section (different water depths along it) and to the manoeuvrability of the  
251 | whole system, only a portion of the section has been sampled. A scheme of the adopted  
252 | multi-sampling system and of its location is reported in Figure 4.

253

#### 254 | *CROSS-FLOW FERT*

255 | Cross-flow FERT has been used as an independent tool for monitoring the  
256 | execution of salt dilution tests and have been executed by means of an array of 16  
257 | underwater electrodes (14 on the canal bottom and 2 on his sides). The electric cable has  
258 | been anchored on the canal bottom by means of appropriate weights and the position of  
259 | each electrode together with the shape of the section has been measured. An example of  
260 | the electrodes disposition scheme for the test site and a picture of the array is reported in  
261 | Figure 5.

262 | The electric cable has been connected to an AC acquiring device (CIT Iridium  
263 | Italy s.a.s.) injecting a sinusoidal current at 916 Hz. The CIT is a very fast acquisition  
264 | device with 16 bit resolution. Indeed the instrument can execute approximately 20  
265 | acquisitions per second (at the selected operative frequency) so that the acquisition of a  
266 | single tomographic image can be performed in a relatively fast time. A devoted  
267 | acquisition sequence consisting of a total of 227 quadrupoles (both dipole-dipole and

268 Wenner types) has been used. In this way it is possible to appreciate variations in  
269 concentration also for relatively fast transient phenomena. The acquisitions have been  
270 performed continuously for about 5 min after the impulse plume has been injected in the  
271 canal. The time required for the acquisition of a single image is of the order of 30  
272 seconds for the experimental setup of this study, including also saving the file and  
273 starting up the new measurement, therefore the total number of processed images, during  
274 the passage of the salt plume, is 9. Data have been inverted by means of an on purpose  
275 designed software (NES Electric Arbitrary 2D Closed Geometry by Andrea Borsic)  
276 which is based on a damped least squares inversion algorithm.

277         A representation based on the relative difference in electric resistivity (ER)  
278 among the several images has been adopted in the following. Reference was made to the  
279 "clear water" condition by subtracting the resistivity distributions obtained at each time  
280 step to a reference image of the canal water measured before the slug injection (ER of 58  
281  $\Omega\cdot\text{m}$  coherently corresponding to the inverse of the directly measured EC [of 170  \$\mu\text{S}/\text{cm}\$](#) ).  
282 In this way the passage of the salt plume is expected to provide an overall reduction in  
283 resistivity (increased concentration of the salt plume) over the images. Indeed ER is the  
284 inverse of EC, so that symmetrical considerations can be made in respect to his  
285 behaviour with increasing salt concentration. The same laboratory calibration curve used  
286 for the salt dilution method has been later used to convert the resistivity maps in salt  
287 concentration maps.

288

289

## RESULTS AND DISCUSSION

The ~~NaCl-measured breakthrough~~ curve ~~of from~~ the direct sampling with the adopted multi-sampling system is reported in Figure 6; ~~for convenience of comparison with the results of cross-flow FERT data have been converted in ER.~~ ~~Given~~ the equations reported in the previous paragraph, this curve highlight a discharge equal to 0.46 m<sup>3</sup>/s. ~~For convenience of comparison with the results of cross flow FERT data have been converted in ER~~ The main peak evidenced from this curve was of about 14  $\Omega$ .m corresponding to an EC of about 700  $\mu$ S/cm, this results in a peak concentration of 0.27 gr/l. ~~and a~~ An indication of the average time of acquisition of each tomographic image is also reported in ~~Figure 6~~ ~~the same figure~~.

The results of some acquired images during the passage of the salt plume are instead presented in Figure 7; some of the images, with very similar ER distribution, have been suppressed (dashed lines in Figure 6) for easiness of visualization. In these images the ER difference with respect to the "clear water" condition (image at time 25 s) are reported. Images are very clear in ~~the recognition of evidencing~~ the passage of the plume, correctly identified with a strong resistivity reduction. This reduction is quite homogeneous in the early times, in correspondence to the higher salt concentration in the transient plume, but appears more concentrated in some zones of the canal in late times. Noticeably the left side of the reconstructed resistivity image (which is upstream the canal curve) appears not affected by the passage of the plume. This has been also observed on site by visual inspection of the passing plume. The imaged reduction in

312 resistivity shows an average values around of about -25 Ω.m in respect to the clear  
313 water, even if localized higher values more marked reductions (around -30 - 35 Ω.m) are  
314 present in the map. These values- average reduction seem as little lower with respect to  
315 the direct sampled curve which instead reports an average peak reduction of about -40  
316 Ω.m reduction with respect to the canal "clear water" resistivity (from 58 Ω.m to about  
317 14 Ω.m Figure 6).

318         The resistivity images acquired have been then interpreted in order to extract  
319 quantitative information about the salt concentration. Such interpreted data are reported  
320 in Figure 8 for the same sampling intervals of Figure 7 and in Figure 9 in a 3D  
321 representation. The leading edge of the salt plume is clearly evidenced in both images  
322 and appears relatively uniform: this suggest that turbulence exists such that mixing is  
323 fairly uniform in early stages. However, with respect to the previous images, in late  
324 times intervals some localized peaks in concentration appear, more evidently related to  
325 the laminar type of flow of the canal. Particularly in the 3D visualization it appears clear  
326 that the "eoda" tailing edges of the plume reveal high concentration zones are located  
327 along the banks of the canal. Since dead zones do not seem to be present in the  
328 measuring reach the result confirm the supposed "sinuous" flow regime. Indeed the  
329 velocity of flow varies from zero at the walls to a maximum along the center as  
330 evidenced also by preliminary qualitative tests by means of a current meter. This  
331 therefore reflects in two main concentration peaks located on both sides of the

332 measuring section and only one of them appears correctly sampled by the direct method  
333 since the sampling grid has been placed nearer to the left downstream bank (Figure 4).

334 By extracting mean and standard deviation values of concentration in every  
335 tomographic image it is also possible to estimate a time-concentration curve also from  
336 geophysical measurements. This interpretation is reported in Figure 10 and compared to  
337 the one obtained from direct measurements. The mass balance of the injected salt  
338 extracted from the two evaluations (i.e. direct sampling and cross-flow FERT) partially  
339 differs, the mean value of cross-flow FERT data report globally a lower concentration  
340 peak (around 0.1 gr/l). There are several reasons ~~to that could~~ explain the observed  
341 differences:

342 - the concentration extracted from cross-flow FERT is an integral concentration  
343 over ~~a the~~ measuring time (~~30 s~~), indeed it takes "all" the 30 s interval to reconstruct an  
344 image since the measuring sequence shifts the different quadrupoles in different  
345 positions along the section during this time interval; ~~which this~~ -is higher than the one  
346 used for direct sampling (5 s); ~~this and~~ will probably result in a reduced peak value  
347 given the fast phenomenon in observation;

348 - the reduced peak concentration observed by cross-flow FERT may be also  
349 related to the smoothing of the inversion algorithm adopted which does not allow for too  
350 sharp variations in conductivity and therefore in concentration. It is worthy to note ; ~~it~~  
351 ~~must indeed be noted~~ the ~~increased dimensions of larger~~ standard deviation error-bars  
352 (which, regardless the statistical distribution of data, are an index of dispersion around  
353 an average value ~~index~~) near the peak of the plume with respect to smaller ones towards



354 the end of it, sign of a more homogeneous situation. ~~towards the end of it; this implies~~  
355 ~~that w~~When the concentration distribution within the section ~~is sharp~~ is more irregular  
356 because of sparse, different concentration values, the inverse solution has increased  
357 variability;

358 - cross-flow FERT conversely images the whole section of the canal (~~included~~  
359 including the left bank zone where there appear to be a reduced concentration area; ~~→~~)  
360 therefore in respect to the direct sampling technique has the potentiality to "sample" the  
361 whole plume distribution and result in a ~~and therefore seems globally~~ more reliable  
362 average visualization of it;

363 - direct sampling can be affected by localized high concentration points, in  
364 correspondence of the sampling grid, which could ~~influence~~ partially bias towards  
365 higher concentrations the overall estimate; indeed if the maximum concentration value is  
366 considered ~~data offrom~~ cross-flow FERT data the curves seems ~~indeed~~ to be better in  
367 agreement ~~if the maximum concentration value is considered~~ (dashed red line in Figure  
368 10);

369 In order to assess the likelihood of this last ~~reason~~ consideration, a comparison  
370 between direct sampling and cross-flow FERT has been performed, over the same  
371 sampling area of the canal (i.e. 0.5 m-1.5 m from left bank). In this respect Figure 11  
372 reports an image of the plume in ~~correspondence of the sampling grid~~ this area at the  
373 time of passage of the main concentration peak. It can be noted that ~~most~~ some of the  
374 spilling points appears located near to high concentration peaks and therefore due to this  
375 and due to the unsampled low concentration left bank zone the average concentration

376 curve may be biased towards higher values. Providing similar images preliminary to the  
377 design of the sampling grid could be therefore a strong help in establishing the most  
378 correct measurement protocol.

379

## 380 **CONCLUSIONS**

381

382 Direct sampling of the NaCl plume from a slug-injection salt dilution test and  
383 geophysical imaging of the same salt plume, by means of cross-flow fast electric  
384 resistivity tomography (FERT), have been compared in this work [in a single case](#)  
385 [history](#). Direct sampling has been performed with a [prototype](#) multisampling  
386 optimization in the downstream section, obtaining an average value over the sampled  
387 [stream-sectionarea](#), using a contemporary water sampling; geophysical data have been  
388 acquired and interpreted independently.

389

390 Results shows that the reconstructed curve from cross-flow FERT seems affected  
391 from an overall lower sensitivity in respect to the peak passage of the plume and  
392 therefore mass balance estimations based on these data cannot be [considered](#) completely  
393 reliable. [At the present development of the geophysical instrumentation, the FERT](#)  
394 [technique indeed still suffer from limitations mainly related to the velocity of acquisition](#)  
395 [and can therefore offer only qualitative representations of the salt plume.](#) Nevertheless  
396 cross-flow FERT has provided a [good-qualitative-reliable](#) visualization of the passage of  
397 the plume in the imaged section [evidencing also some localized low conductivity zones.](#)  
[and, s](#)Since the knowledge of tracer distribution in the [measuring](#) cross-section is very

398 important for a correct location of sampling points, FERT can be potentially used as a  
399 preliminary control in ~~order to establish the best position for accurate discharge~~  
400 ~~measurements by means of the direct sampling method~~this respect.

401 ~~Following this first visualization, a sampling optimization in the downstream~~  
402 ~~sampling section, using a multisampling technique, can be strongly recommended. This~~  
403 ~~method, sampling the canal water in different points of the cross section, by means of a~~  
404 ~~contemporary water picking up, can indeed optimize the quantitative detection and result~~  
405 ~~in more reliable discharge estimates.~~

406 Indeed, discharge measurements by means of the salt dilution method is the most  
407 used approach especially in difficult to access areas: in these situations tests precautions  
408 can fight with logistical conditions and it is not always easy to establish a priori whether  
409 all the test requirements are satisfied. Geophysical imaging can be therefore an  
410 important aid offering a direct visualization of the salt plume and consequently a more  
411 correct location of sampling points. Following this first visualization, a sampling  
412 optimization in the downstream sampling section, using a multisampling technique, can  
413 be strongly recommended. Sampling the canal water in different points of a cross  
414 section, by means of a contemporary water picking up, can optimize the quantitative  
415 detection and results in more reliable discharge estimate.

416 We are conscious that the single case history presented has to be considered  
417 only as a starting point both for the FERT technique and for the multisampling prototype  
418 apparatus. Further tests in other conditions and different flow regimes are planned to  
419 result in a more consistent discussion on the topic. Nevertheless the presented case

420 | [history offers a clear delineation of the potentiality of the presented methodology to be](#)  
421 | [viewed as a developing point also for other researchers.](#)

422

### 423       **ACKNOWLEDGMENTS**

424

425           This research has been partially funded in the framework of a research project  
426 between the Agricultural Management of Piedmont Region and the Earth Science  
427 Department of Università degli Studi di Torino. Authors are indebted with Paolo  
428 Clemente, Giovanna Dino, Diego Franco, Francesco Marzano and Sabrina Bonetto for  
429 their help in the execution of the field tests.

430

431

432

433 **REFERENCES**

434

435 Clemente, P., De Luca, D. A., Dino, G. A., and Lasagna, M.: Water losses from  
436 irrigation canals evaluation: comparison among different methodologies, Geophys.  
437 Res. Abstr., EGU2013-9024, EGU General Assembly 2013, Vienna, Austria,  
438 2013.

439 Day, T. J.: On the precision of salt dilution gauging, *J. Hydrol.*, 31, 293–306, 1976.

440 Drost, J. W.: Single-Well and Multi-Well Nuclear Tracer Techniques – a Critical  
441 Review, Technical Documents in Hydrology, International Hydrological  
442 Programme, 96, UNESCO, Paris, 1989.

443 Fangary, Y. S., Williams, R. A., Neil, W. A., Bond, J., and Faulks, I.: Application of  
444 electric resistance tomography to detect deposition in hydraulic conveying  
445 systems, *Powder Technol.*, 95, 61–66, 1998.

446 Gees, A.: Flow measurement under difficult measuring conditions: Field experience  
447 with the salt dilution method, in: *Hydrology in Mountainous Regions I. Hydrological Measurements; The Water Cycle*, edited by: Lang, H. and Musy, A.,  
448 IAHS Publ., 193, 255–262, 1990.

449  
450 [Hudson, R. and J. Fraser. 2002. Alternative methods of flow rating in small coastal  
451 streams. B.C. Ministry of Forests, Vancouver Forest Region. Extension Note EN-  
452 014 Hydrology. 11 p.](#)

453 [Jaramillo F. \(2007\). Estimating and modeling soil loss and sediment yield in the  
454 Maracas-St. Joseph River Catchment with empirical models \(RUSLE and  
455 MUSLE\) and a physically based model \(Erosion 3D\). Master in Civil Engineering-  
456 Thesis. McGill University, 134 pp.](#)

457

458 Kalbus, E., Reinstorf, F., and Schirmer, M.: Measuring methods for groundwater –  
459 surface water interactions: a review, *Hydrol. Earth Syst. Sci.*, 10, 873–887,  
460 doi:10.5194/hess-10-873-2006, 2006.

461 [Kite, G. 1993. Computerized streamflow measurement using slug injection.  
462 Hydrological Processes 7:227–233.](#)

463

464 Kumar, B. and Nachiappan, R. P.: Estimation of alluvial aquifer parameters by a single-  
465 well dilution technique using isotopic and chemical tracers: a comparison, in:  
466 Tracers and Modelling in Hydrogeology, IAHS Publ. 262, edited by: Dassargues,  
467 A., IAHS Press, Wallingford, 53–56, 2000.

468 Lucas, G. P., Cory, J., Waterfall, R. C., Loh, W. W., and Dickin, F. J.: Measurement of  
469 the solids volume fraction and velocity distributions in solids–liquid flows using  
470 dual-plane electrical resistance tomography, *Flow Meas. Instrum.*, 10, 249–258,  
471 1999.

472 Moore, R. D.: Slug injection using salt in solution, *Streamline Watershed Management  
473 Bulletin*, 8, 1–6, 2005.

474 [Moore, R.D. 2004. Introduction to salt dilution gauging for streamflow measurement:  
475 Part I. Streamline Watershed Management Bulletin 7\(4\):20–23.](#)

476 |  
477 Perotti, L., Clemente, P., De Luca, D. A., Dino, G. A., and Lasagna, M.: Remote sensing  
478 and hydrogeological methodologies for irrigation canal leakage detection: the  
479 Osasco and Fossano test sites (Northwestern Italy), *Geophys. Res. Abstr.*,  
480 EGU2013-5705, EGU General Assembly 2013, Vienna, Austria, 2013.

481 Radulovic, M., Radojevic, D., Devic, D., and Blecic, M.: Discharge calculation of the  
482 spring using salt dilution method – application site Bolje Sestre Spring  
483 (Montenegro), available at: [http: 25 //balwois.com/balwois/administration](http://25//balwois.com/balwois/administration/full_paper/ffp-1257.pdf)  
484 [/full\\_paper/ffp-1257.pdf](http://25//balwois.com/balwois/administration/full_paper/ffp-1257.pdf) (last access: 24 July 2013), 2008.

485 Rantz, S. E.: *Measurement and Computation of Streamflow: Volume 1. Measurement of*  
486 *Stage and Discharge*, US Geological Survey Water-Supply Paper 2175, US  
487 Department of the Interior, US Government Printing Office, Washington, DC,  
488 1982.

489 Sambuelli, L. and Comina, C.: Fast ert to estimate pollutants and solid transport  
490 variation in water flow: a laboratory experiment, *B. Geofis. Teor. Appl.*, 51, 1–22,  
491 2010.

492 Sambuelli, L., Lollino, G., Morelli, G., Socco, L. V., and Bidone, L.: First experiments  
493 on solid transport estimation in river-flow by fast impedance tomography, VIII  
494 EEGS meeting, 8–15 September, cd-rom 4 pp., Aveiro, Portugal, 2002.

495 [Scobey F.C. \(1939\). Flow of water in irrigation and similar canals. U.S. Dept. of](#)  
496 [Agriculture. Pp. 79](#)

497 Tapp, H. S. and Wilson, R. H.: Developments in low-cost electrical imaging techniques,  
498 *Process Contr. Qual.*, 9, 7–16, 1997.

499 Tazioli, A.: Experimental methods for river discharge measurements: comparison among  
500 tracers and current meter, *Hydrolog. Sci. J.*, 56, 1314–1324, 2011.

501 Xie, C. G., Reinecke, N., Beck, M. S., Mewes, D., and Williams, R. A.: Electrical  
502 tomography techniques for process engineering applications, *Chem. Eng. J.*, 56,  
503 127–133, 1995.

504 Wang, M. and Cilliers, J. J.: Detecting non-uniform foam density using electrical  
505 resistance tomography, *Chem. Eng. Sci.*, 54, 707–712, 1999.

506 Warsito, W. and Fan, L. S.: Measurement of real-time flow structures in gas–liquid and  
507 gas–liquid–solid flow systems using electrical capacitance tomography (ECT),  
508 *Chem. Eng. Sci.*, 56, 6455–6462, 2001.

509 Yang, W. Q. and Liu, S.: Role of tomography in gas/solids flow measurement, *Flow*  
510 *Meas. Instrum.*, 11, 237–244, 2000.

511 |  
512 |  
513 |  
514 |  
515 |  
516 |  
517 |  
518 |  
519 |

520 **FIGURE CAPTIONS**

521  
522  
523 **Figure 1.** Geographical location of the test canal (inlet) and a more detailed view  
524 in the proximity of the test site.

525  
526 **Figure 2.** Tested canal reach: a) injection point at the end of a cemented weir and  
527 b) measuring section, under a small road bridge and before a canal curve.

528  
529 **Figure 3.** Calibration curve for converting EC measured data to concentration  
530 values with reference to the natural water electrical conductivity ( $170 \mu\text{S}/\text{cm}$ ).

531  
532 **Figure 4.** Multi-sampling system with details of the sampling grid (black circles  
533 are water spilling points) and of the pumping apparatus; the below section is seen from  
534 up-stream.

535  
536 **Figure 5.** Electrodes disposition for cross-flow FERT: images of the electrodes  
537 and the anchoring system (top) and of the mesh used for the inversion (bottom), the  
538 below section is seen from up-stream.

539  
540 **Figure 6.** Time-resistivity curve determined with the multisampling apparatus  
541 and indication of the number and time of execution of the cross-flow FERT images  
542 presented in Figure 7 and 8 (full lines).

543  
544 **Figure 7.** Electric resistivity differences in the imaged section for increasing  
545 times, image number with reference to Figure 6, seen from up-stream.

546  
547 **Figure 8.** Incremental concentrations in the imaged section for increasing times,  
548 image number with reference to Figure 6, seen from up-stream.

549  
550 **Figure 9.** 3D visualization of the passage of the salt plume in the studied canal  
551 section, [time axis coherent with figure 6.-](#)

552  
553 **Figure 10.** Comparison of direct sampling and cross-flow FERT obtained  
554 concentration curves; the dashed red line refers to the maximum concentration value  
555 determined from cross-flow FERT in the area of the canal reported in Figure 11.

556  
557 **Figure 11.** Comparison of direct sampling (black circles are water spilling  
558 points) and cross-flow FERT over the same sampling area at the time of passage of the  
559 main plume.

560  
561  
562

563 **FIGURE 1**

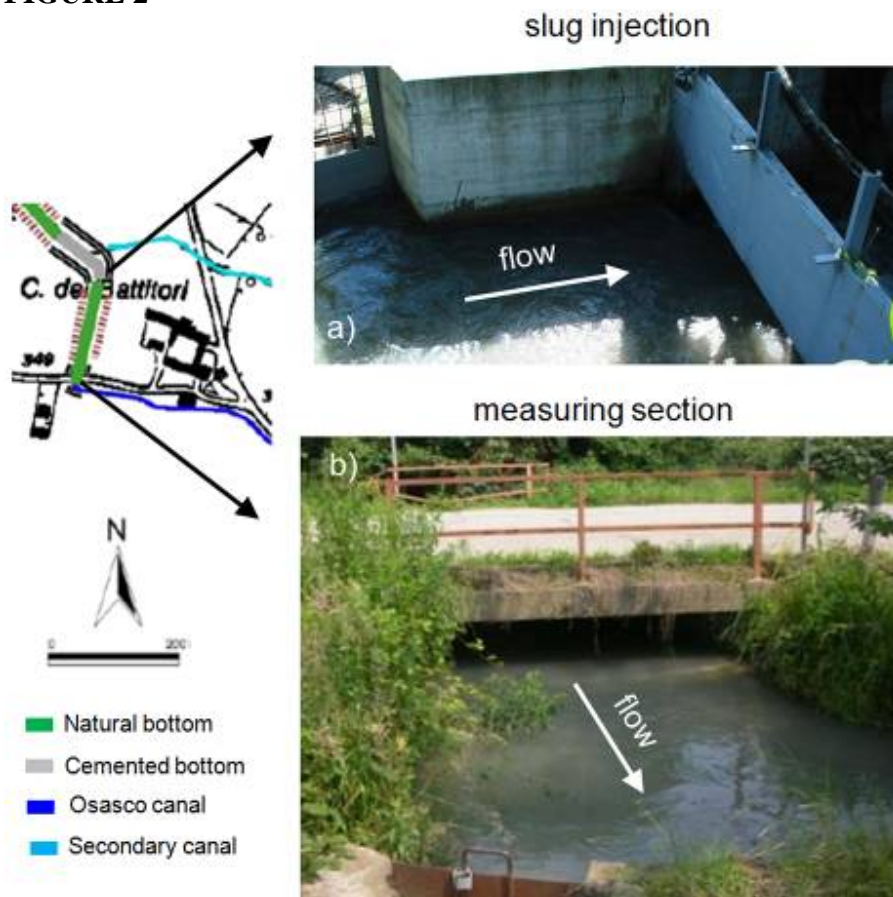


564

565

566

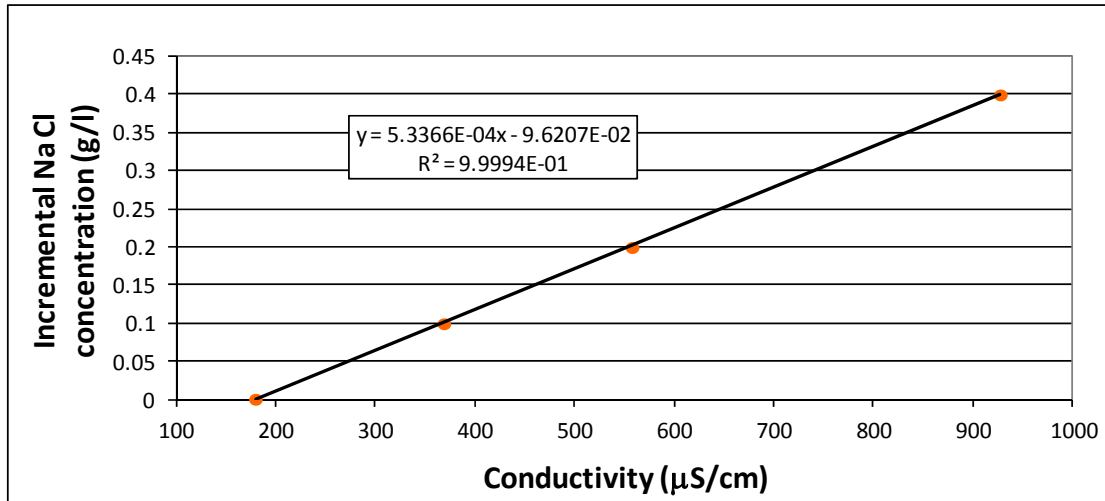
**FIGURE 2**



567



568 **FIGURE 3**

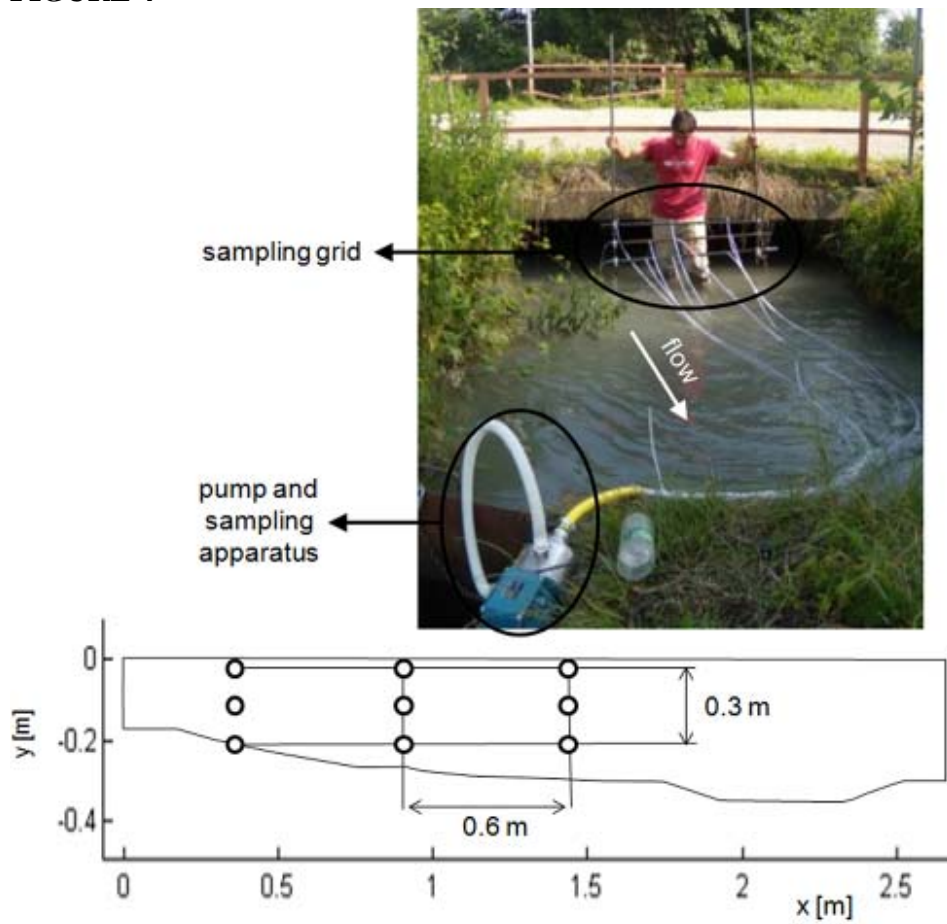


569

570

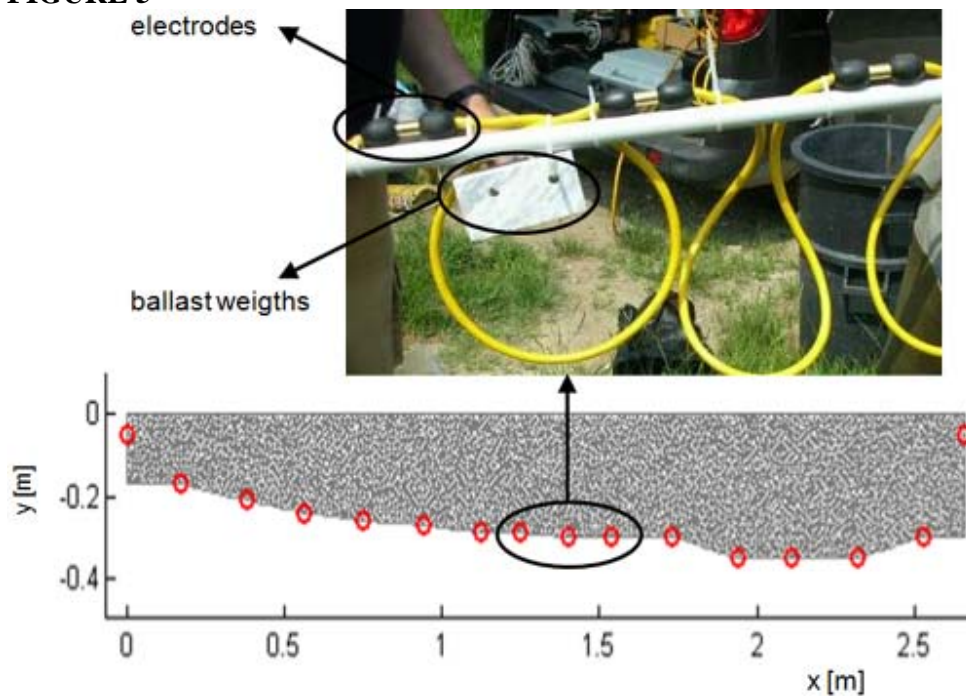
571

**FIGURE 4**



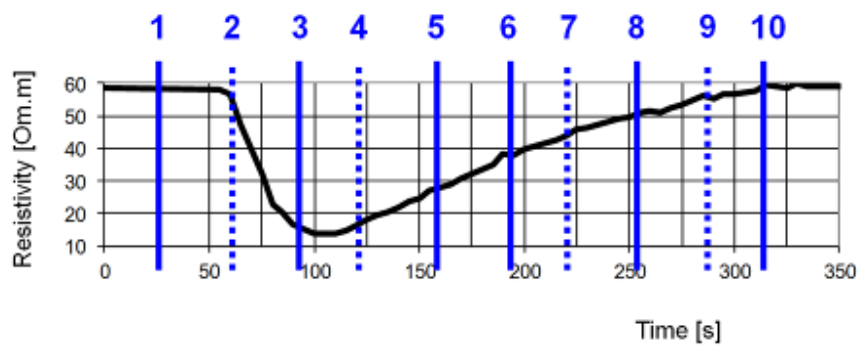
572

573 **FIGURE 5**



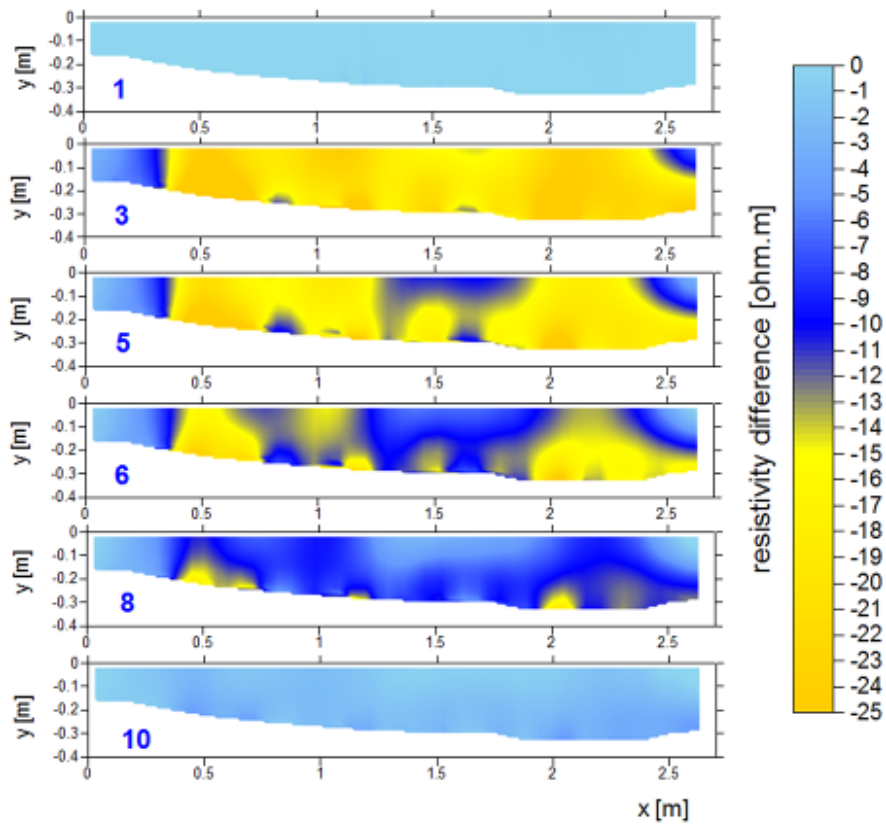
574  
575  
576

**FIGURE 6**



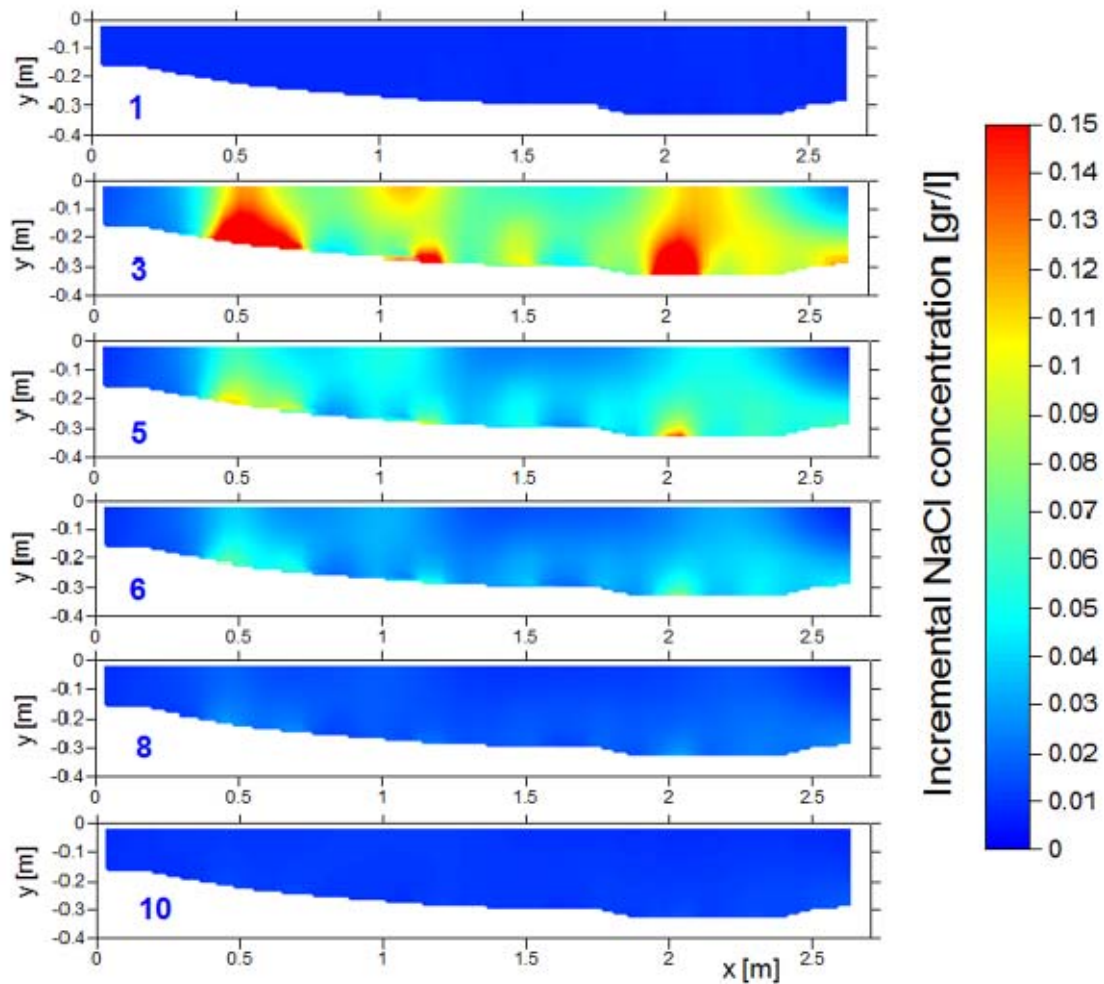
577  
578

579 **FIGURE 7**  
580



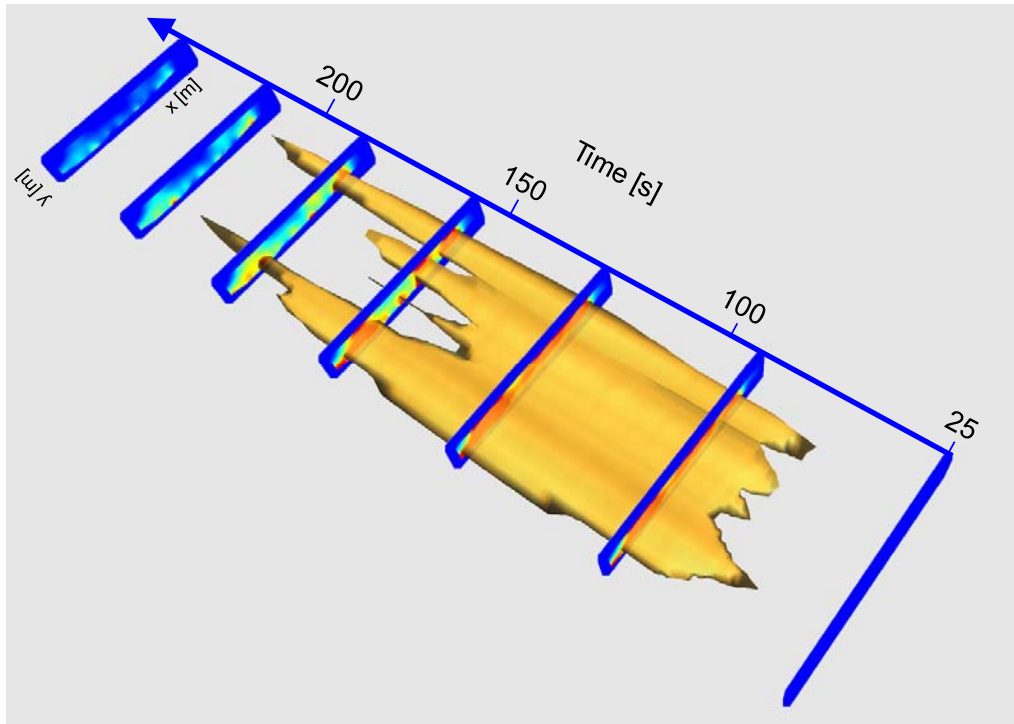
581  
582

583 **FIGURE 8**



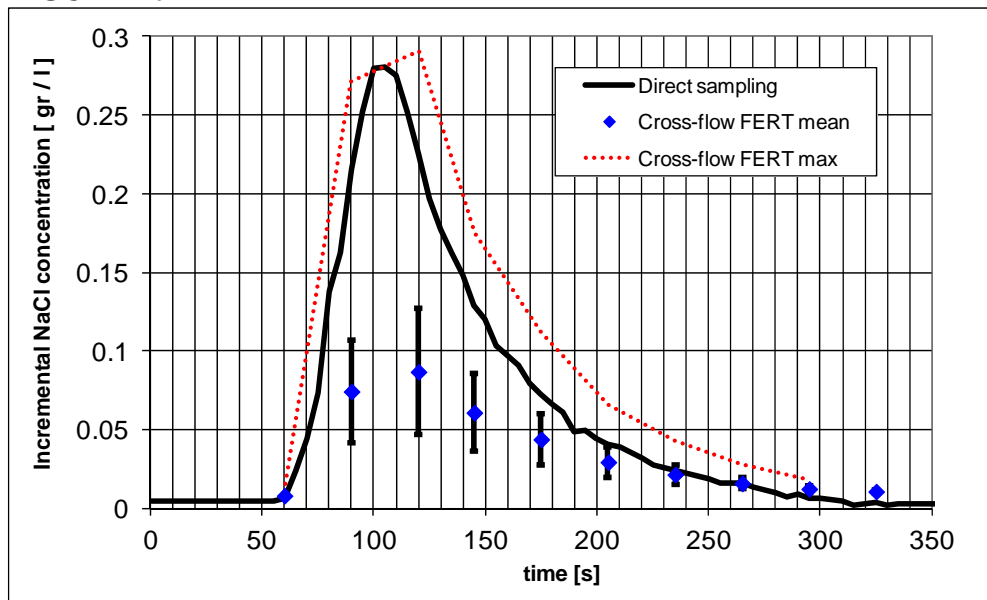
584  
585

586 **FIGURE 9**



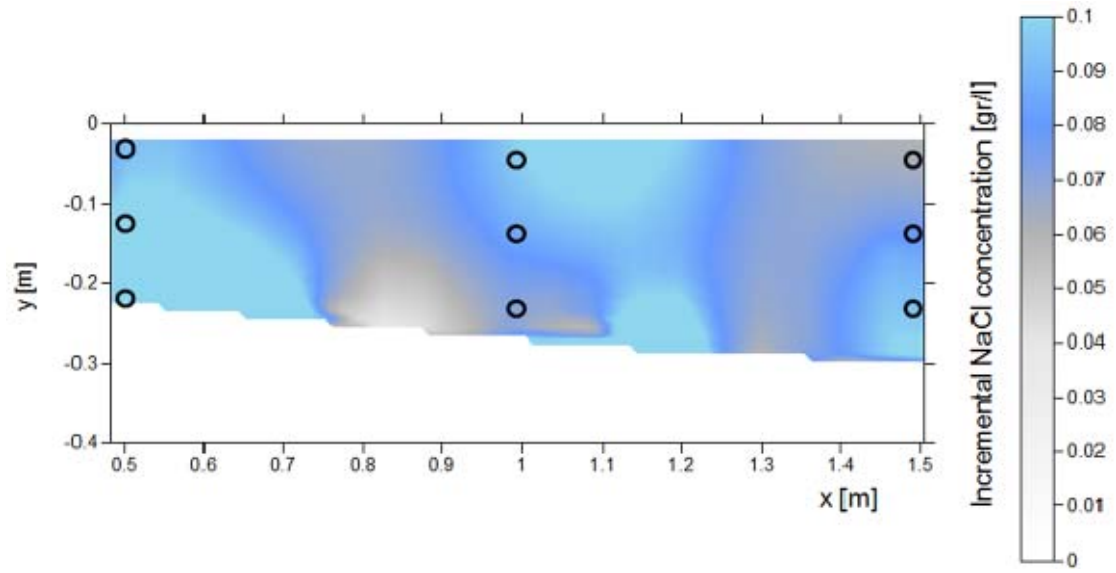
587  
588  
589  
590

**FIGURE 10**



591  
592

593 **FIGURE 11**



594  
595  
596